Ferroelectric switching: a micromechanics model versus measured behaviour

J.E. Huber [*], N.A. Fleck

Department of Engineering, University of Cambridge, Trumpington Street, Cambridge CB2 1PZ, UK

Abstract

The behaviour of ferroelectric polycrystals is explored using a rate-independent crystal plasticity model with self-consistent homogenisation to capture grain–grain interactions. Dimensionless parameters are introduced that allow a simple connection to be made between material constants and the nonlinear ferroelectric behaviour. In particular, combinations of material parameters are identified that cause remanent straining to be strongly suppressed. The self-consistent scheme allows for the ferroelectric response of a composite of grains with distinct sets of switching systems to be modelled. This feature is used to explore the effect of pinned domain walls and of dielectric inclusions. The model is able to reproduce the electrical response of three materials (PZT-5H, PZT-4D and Barium Titanate) under proportional stress and electric field loading, as measured in a parallel study.
© 2003 Elsevier SAS. All rights reserved.

Keywords: Ferroelectric material; Micromechanical model; Self-consistent

1. Introduction

Models of ferroelectric switching in polycrystals have been widely used to predict the non-linear response of piezoelectric and ferroelectric devices and to study the local effects of cracks and embedded electrodes. A significant difficulty arises with models of ferroelectricity in that the materials exhibit a complicated history dependence. This behaviour is captured in models by internal state variables: the rates of strain and polarization are then functions of the applied loads, and of the internal variables. A single scalar internal variable provides sufficient complexity to capture many of the phenomena found in ferroelectrics, such as dielectric hysteresis, butterfly hysteresis in strain versus electric field, and depolarization by compressive stress. However, a greater degree of complexity is necessary in order to reproduce multi-axial behaviour.

There is a wide range of ferroelectric behaviour: "hard" compositions have low hysteresis and high coercive field and Curie Temperature, whilst "soft" compositions typically have high hysteresis, but low coercive field and Curie Temperature. At present no model in the literature has been tested across the full range of behaviour. Several authors have presented models which reproduce qualitatively the main ferroelectric phenomena under uniaxial mechanical and electrical loading (see, for example, Hwang et al., 1995; Lynch, 1998; Kamlah and Jiang, 1999; Michelitsch and Kreher, 1999; Huber et al., 1999). Studies also exist that attempt a quantitative match to measured data, both using uniaxial test data (Bassiouny and Maugin, 1989; Arlt, 1996a; Chen et al., 1997; Hwang et al., 1998; Li and Weng, 1999; Fan et al., 1999) and using multi-axial test data (Huber and Fleck, 2001; Landis, 2002).

An emerging issue is the calibration of models to reproduce with reasonable accuracy the multi-axial, coupled material response. In phenomenological schemes it is possible, in principle, to use a measured bulk material response, such as the electric displacement versus electric field during poling, as a direct input to the model (see for example the calibration

---

discussed by Haug et al., 2003). Consequently, the model reproduces the input data exactly, and may reproduce the response to other types of loading accurately if the underlying physics embedded in the model is sufficiently realistic. In the present study a micromechanical model is used: the macroscopic response to any given loading case is calculated on the basis of a set of micromechanical parameters, which are, ideally, measured directly. If the model fails to reproduce the material response it follows that either the underlying physics, or the set of parameters, or both are incorrect. In practice the set of required parameters are not readily available, and the measurements themselves present practical difficulties. Consequently, it is necessary to fit the micromechanical models to available material measurements, making use of approximate material parameters.

This work is an attempt at using an existing crystal plasticity model to reproduce measured material responses for three different materials under combined stress and electrical loads. A self-consistent scheme is used to represent polycrystal behaviour, for an isotropic distribution of grains, following Huber et al. (1999). The ability of the model to reproduce quantitatively the electrical response of hard PZT-4D, soft PZT-5H compositions and of Barium Titanate ceramic is assessed. The ability of a closely related approach to model Barium Titanate under electrical loading has already been demonstrated by Landis and McMeeking (2001).

In this study, the effect of varying each of the principal model parameters is discussed; dimensionless groups are identified which govern the observed material behaviour. Additionally, attention is given to the influence of the set of switching systems on the macroscopic response. It is shown that the set of switching systems dictates the macroscopic hardening and saturation behaviour of the polycrystal.

A useful feature of the micromechanical model employed here is the flexibility to freeze (i.e., to prevent from becoming active) any subset of transformations; this reproduces in the model the absence, or pinning, of the corresponding domain walls. Furthermore, it is straightforward to model the effects of dielectric inclusions which modify the bulk ferroelectric response. This allows the model to include the effect of "dead" material that has dielectric and elastic properties similar to the bulk, but does not undergo ferroelectric switching.

By combining appropriate choices of model parameters and crystal system, the behaviour of a variety of polycrystalline ferroelectrics is reproduced quantitatively within the same framework.

2. Model description

All calculations of material response in the present study are carried out using the rate-independent crystal plasticity model formulated by Huber et al. (1999). The physical description which forms the basis of this model is that the remanent strain ε^r and the remanent polarization $\mathbf{P}^r$ in ferroelectric crystals arise due to the presence of ferroelectric domains, which are regions of uniform polarization and remanent strain. The domain walls, which separate adjacent domains, may move under a driving force and consequently convert material from one domain into part of an adjacent domain. The resulting changes in remanent quantities are seen macroscopically as ferroelectric or ferroelastic switching.

At the level of a single crystal, the average strain ε and electric displacement $\mathbf{D}$ are decomposed into an "elastic" part (including linear elastic, piezoelectric and dielectric response) that is linearly dependent on the current stress σ and electric field $\mathbf{E}$, and a remanent part ($\varepsilon^r, \mathbf{P}^r$), so that:

$$\begin{bmatrix} \varepsilon \\ \mathbf{D} \end{bmatrix} = \begin{bmatrix} \mathbf{S} & \mathbf{d} \\ \mathbf{d} & \kappa \end{bmatrix} \begin{bmatrix} \sigma \\ \mathbf{E} \end{bmatrix} + \begin{bmatrix} \varepsilon^r \\ \mathbf{P}^r \end{bmatrix}, \tag{1}$$

where $\mathbf{S}$ is the fourth order tensor of elastic moduli, $\mathbf{d}$ the third order piezoelectric tensor, and κ the second order dielectric tensor. The stress σ and electric field $\mathbf{E}$ are assumed to be uniform throughout the single crystal for simplicity. Note that adjacent domains may experience significant clamping stresses and electric fields for some arrangements of domain walls, in which case the assumption of uniform fields is poor. In practice, however, domain walls typically form in compatible arrangements, which minimise energy and thus keeping clamping stresses low (Shu and Bhattacharya, 2001). This motivates the assumption of uniform stress and electric field at the single crystal level, with compatible discontinuities in strain and electric displacement.

The aim is to find instantaneous tangent moduli for each crystal, with tangent moduli defined by:

$$\begin{bmatrix} \dot{\varepsilon} \\ \dot{\mathbf{D}} \end{bmatrix} = \begin{bmatrix} \mathbf{S}^t & \mathbf{d}^t \\ \mathbf{d}^t & \kappa^t \end{bmatrix} \begin{bmatrix} \dot{\sigma} \\ \dot{\mathbf{E}} \end{bmatrix}, \tag{2}$$

where dots indicate the rates of various quantities and superscript "t" indicates tangent quantities.

Although the elastic and dielectric moduli $\mathbf{S}$ and κ are typically anisotropic in ferroelectric crystals, the principal source of anisotropy is in the piezoelectric moduli. In the present study, the approximation is made that $\mathbf{S}$ and κ are isotropic and identical in each domain, with shear modulus μ, Poisson's ratio ν and dielectric constant κ:

$$S_{ijkl} = \frac{1}{4\mu}\left(\delta_{ik}\delta_{jl} + \delta_{jk}\delta_{il} - \frac{2\nu}{1+\nu}\delta_{ij}\delta_{kl}\right), \tag{3}$$

$$\kappa_{ij} = \kappa\delta_{ij}, \tag{4}$$

where δ is the Kronecker delta. Consequently, there is no change in either $\mathbf{S}$ or κ due to switching. The piezoelectric response is approximated by transversely isotropic piezoelectricity for each domain (this is exact for tetragonal crystals of symmetry 4 mm):

$$d_{ijk} = (d_{33})n_i n_j n_k + (d_{31})(n_i\delta_{jk} - n_i n_j n_k) + \frac{1}{2}(d_{15})(\delta_{ij}n_k - 2n_i n_j n_k + \delta_{ik}n_j), \tag{5}$$

where $\mathbf{n}$ is a unit vector in the polarization direction for the crystal variant. For simplicity, in the present work, two approximations are made regarding the piezoelectric constants d_{33}, d_{31} and d_{15}. First, the piezoelectric shear constant d_{15} is set to zero. Second, upon noting that the remaining two piezoelectric coefficients may be related by:

$$d_{31} = -\frac{\alpha}{2}d_{33}, \tag{6}$$

where α is a dimensionless constant, the approximation $\alpha = 1$ is made. As a result, the piezoelectric response is independent of hydrostatic stress. For many materials, even those used under hydrostatic conditions, α is reasonably close to unity. Calculations indicate that the model is relatively insensitive to the particular choice of d_{15} and d_{31} for the loading under consideration. The approximations simplify the piezoelectric response to a single scalar parameter, and the influence of piezoelectricity on the nonlinear response can thereby be studied in a straightforward way. Neglecting d_{15} is reasonable in the present work only because shear loading cases are not considered. For more general loading, the alternative approximation $d_{15} = d_{33} - d_{31}$ could be used with reasonable accuracy for many materials.

Note that the linear elastic, dielectric and piezoelectric coefficients can be represented by a 9×9 matrix, relating the 9 independent load components (6 of stress and 3 of electric field) to the corresponding 9 components of strain and electric displacement. In the present formulation the resulting stiffness matrix depends on only 5 coefficients: two elastic moduli (for example the shear modulus μ and Poisson's ratio ν) the dielectric permittivity κ, and piezoelectric coefficients d_{33} and α as defined by Eq. (6).

Positive electromechanical strain energy is ensured for linear states of loading provided that the stiffness matrix is positive definite. This dictates the constraint

$$\frac{\mu d_{33}^2}{\kappa}\left(\frac{2 - 2\nu + \alpha^2 - 4\alpha\nu}{1 - 2\nu}\right) < 1. \tag{7}$$

For the choice $\alpha = 1$ this constraint reduces to

$$d^* \equiv d_{33}\sqrt{3\mu/\kappa} < 1. \tag{8}$$

Note that the dimensionless parameter d^* introduced in Eq. (8) is closely analogous to the electromechanical coupling coefficient (k_{33}) commonly used to characterise piezoelectric materials.

In a crystal containing M distinct crystal variants, with c_I being the volume fraction of the Ith variant, the remanent quantities are assumed to take on volume average values given by

$$\begin{bmatrix} \boldsymbol{\varepsilon}^r \\ \mathbf{P}^r \end{bmatrix} = \sum_1^M c_I \begin{bmatrix} \boldsymbol{\varepsilon}_I \\ \mathbf{P}_I \end{bmatrix}, \tag{9}$$

where $\boldsymbol{\varepsilon}_I$ and $\mathbf{P}_I$ are the remanent strain and polarization of the Ith variant. A consequence of the assumption of uniform stress and electric field *within each crystal* is that the linear moduli of the crystal are given by the volume average of the corresponding moduli for each variant. Since the elastic and dielectric moduli are taken to be isotropic, and thus identical for all variants, only the piezoelectric tensor $\mathbf{d}_I$ of each variant differs. Averaging of the piezoelectric tensor gives:

$$\mathbf{d} = \sum_1^M c_I \mathbf{d}_I. \tag{10}$$

Relations 9 and 10 can be rewritten in incremental form as:

$$\begin{bmatrix} \dot{\boldsymbol{\varepsilon}}^r \\ \dot{\mathbf{P}}^r \end{bmatrix} = \sum_1^M \dot{c}_I \begin{bmatrix} \boldsymbol{\varepsilon}_I \\ \mathbf{P}_I \end{bmatrix} = \sum_{\alpha=1}^N \dot{f}_\alpha \begin{bmatrix} \Delta\boldsymbol{\varepsilon}_\alpha \\ \Delta\mathbf{P}_\alpha \end{bmatrix}, \tag{11}$$

$$\dot{\mathbf{d}} = \sum_1^M \dot{c}_I \mathbf{d}_I = \sum_{\alpha=1}^N \dot{f}_\alpha \Delta\mathbf{d}_\alpha. \tag{12}$$

Here, the right-hand side expresses the rates as sums over the set of N transformation systems α, where $\dot{f}_\alpha$ is the rate of volume fraction transfer associated with system α. The quantity $\Delta\boldsymbol{\varepsilon}_\alpha$ is the change in remanent strain $\boldsymbol{\varepsilon}_I - \boldsymbol{\varepsilon}_J$ caused by transformation system α converting material from variant J to variant I; $\Delta\mathbf{P}_\alpha$ and $\Delta\mathbf{d}_\alpha$ are defined similarly. The N transformation systems are defined such that $\dot{f}_\alpha \geqslant 0$; forward and reverse transformation correspond to the operation of two distinct systems. Given M distinct crystal variants, each of which may transform to each other variant, there are in total $N = M(M-1)$ transformation systems.

When the elastic and dielectric moduli are isotropic and homogeneous within each crystal, the driving force for volume fraction transfer by each transformation system may be written as (Huber and Fleck, 2001; Kessler and Balke, 2001)

$$G_\alpha = \boldsymbol{\sigma} \cdot \Delta\boldsymbol{\varepsilon}_\alpha + \mathbf{E} \cdot \Delta\mathbf{P}_\alpha + \boldsymbol{\sigma} \cdot \Delta\mathbf{d}_\alpha \cdot \mathbf{E}. \tag{13}$$

Transformation on system α occurs only when the driving force G_α reaches a critical value $G_{\alpha c}$. During transformation the conditions

$$G_\alpha = G_{\alpha c}, \quad \dot{G}_\alpha = \dot{G}_{\alpha c}, \quad \dot{f}_\alpha > 0 \quad \text{and} \quad c_J > 0 \tag{14}$$

are satisfied for transformation system α, where c_J is the current volume fraction of the variant depleted by system α. The condition $c_J > 0$ ensures the saturation of switching when the volume fraction of variant J is completely depleted. The constitutive description of the crystal is completed by relating the increments in $\dot{G}_{\alpha c}$ to the transformation rates $\dot{f}_\alpha$ via a hardening law. For simplicity, independent hardening is adopted, with

$$\dot{G}_{\alpha c} = h\dot{f}_\alpha \tag{15}$$

in terms of a constant hardening parameter h. The hardening rule (15) does not represent a real hardening process – ferroelectrics typically give a stable cyclic hysteresis, suggesting that in practice isotropic hardening is negligible. The calculations presented below neglect hardening by taking h to be sufficiently small to approximate the limit $h \to 0$. The effect of a small value of $h/G_{\alpha c}$ upon the model response is discussed in Section 3.1.

The tangent moduli of the crystal, as defined by Eq. (2), are derived as follows. Expressing Eq. (1) in rate form, and making use of Eqs. (11) and (12) gives

$$\begin{bmatrix} \dot{\boldsymbol{\varepsilon}} \\ \dot{\mathbf{D}} \end{bmatrix} = \begin{bmatrix} \mathbf{S} & \mathbf{d} \\ \mathbf{d} & \boldsymbol{\kappa} \end{bmatrix} \begin{bmatrix} \dot{\boldsymbol{\sigma}} \\ \dot{\mathbf{E}} \end{bmatrix} + \sum_\alpha \dot{f}_\alpha \begin{bmatrix} \hat{\boldsymbol{\varepsilon}}_\alpha \\ \widehat{\mathbf{P}}_\alpha \end{bmatrix}, \tag{16}$$

where

$$\hat{\boldsymbol{\varepsilon}}_\alpha = \Delta\boldsymbol{\varepsilon}_\alpha + \Delta\mathbf{d}_\alpha \cdot \mathbf{E}, \tag{17}$$

$$\widehat{\mathbf{P}}_\alpha = \Delta\mathbf{P}_\alpha + \Delta\mathbf{d}_\alpha \cdot \boldsymbol{\sigma}. \tag{18}$$

Combining the hardening law (15) and the driving force for transformation (13) gives

$$\dot{G}_{\alpha c} = h\dot{f}_\alpha = \begin{bmatrix} \hat{\boldsymbol{\varepsilon}}_\alpha & \widehat{\mathbf{P}}_\alpha \end{bmatrix} \begin{bmatrix} \dot{\boldsymbol{\sigma}} \\ \dot{\mathbf{E}} \end{bmatrix}. \tag{19}$$

Finally, eliminating the transformation rates $\dot{f}_\alpha$ from Eqs. (16) and (19) gives

$$\begin{bmatrix} \dot{\boldsymbol{\varepsilon}} \\ \dot{\mathbf{D}} \end{bmatrix} = \left\{ \begin{bmatrix} \mathbf{S} & \mathbf{d} \\ \mathbf{d} & \boldsymbol{\kappa} \end{bmatrix} + \frac{1}{h} \sum_\alpha \begin{bmatrix} \hat{\boldsymbol{\varepsilon}}_\alpha\hat{\boldsymbol{\varepsilon}}_\alpha & \hat{\boldsymbol{\varepsilon}}_\alpha\widehat{\mathbf{P}}_\alpha \\ \widehat{\mathbf{P}}_\alpha\hat{\boldsymbol{\varepsilon}}_\alpha & \widehat{\mathbf{P}}_\alpha\widehat{\mathbf{P}}_\alpha \end{bmatrix} \right\} \begin{bmatrix} \dot{\boldsymbol{\sigma}} \\ \dot{\mathbf{E}} \end{bmatrix}. \tag{20}$$

The item in curly brackets provides the values of the tangent moduli introduced in Eq. (2):

$$\begin{bmatrix} \mathbf{S}^t & \mathbf{d}^t \\ \mathbf{d}^t & \boldsymbol{\kappa}^t \end{bmatrix} \equiv \begin{bmatrix} \mathbf{S} & \mathbf{d} \\ \mathbf{d} & \boldsymbol{\kappa} \end{bmatrix} + \frac{1}{h} \sum_\alpha \begin{bmatrix} \hat{\boldsymbol{\varepsilon}}_\alpha\hat{\boldsymbol{\varepsilon}}_\alpha & \hat{\boldsymbol{\varepsilon}}_\alpha\widehat{\mathbf{P}}_\alpha \\ \widehat{\mathbf{P}}_\alpha\hat{\boldsymbol{\varepsilon}}_\alpha & \widehat{\mathbf{P}}_\alpha\widehat{\mathbf{P}}_\alpha \end{bmatrix}. \tag{21}$$

In Eqs. (20) and (21) the summation over transformation systems α includes only those systems satisfying the conditions (14).

The tangent moduli of a polycrystal of randomly oriented grains may be estimated by averaging the single crystal response over all crystallographic orientations, using a suitable homogenisation procedure. In the present work, a self-consistent scheme is adopted, following Hill (1965) and Huber et al. (1999).

3. Influence of the model parameters

The macroscopic response can be calculated for any given geometric arrangement of switching systems, and for any material parameters as defined above. In the present section, the full set of parameters required to define the crystal system and material properties are enumerated. Where possible, simplifications are made to reduce the number of independent parameters. The material parameters fall into three groups as follows.

(i) The linear moduli of a domain. The linear elastic and dielectric moduli are assumed to be isotropic and can be described using three parameters, the shear modulus μ, Poisson's ratio ν and the dielectric permittivity κ. For the materials under consideration, Poisson's ratio is typically close to 1/3 and small variations in Poisson's ratio do not have a significant effect on the material response. For simplicity, ν is set to 1/3 throughout. The linear piezoelectric response of the domain may be described using three parameters d_{33}, d_{31} and d_{15} for tetragonal crystals of symmetry 4 mm, following Eq. (5). Motivated by the discussion in Section 2, we set d_{15} to zero and $d_{31} = -\alpha d_{33}/2$ with $\alpha = 1$. Thus only the three moduli μ, κ and d_{33} are required.

(ii) The nonlinear parameters for a crystal. For each domain, the lattice strain $\boldsymbol{\varepsilon}_I$ and polarization $\mathbf{P}_I$ must be specified. If $\mathbf{n}$ is a unit vector in the polarization direction for the domain, we set $\mathbf{P}_I = P_0 \mathbf{n}$, where P_0 is the polarization magnitude for a domain. In both the tetragonal and the rhombohedral (trigonal) systems, the lattice strain $\boldsymbol{\varepsilon}_I$ is given by

$$\boldsymbol{\varepsilon}_I = \frac{\varepsilon_0}{2}(3\mathbf{nn} - \boldsymbol{\delta}), \tag{22}$$

where ε_0 is a scalar characterising the magnitude of the lattice strain. In a tetragonal crystal, with one axis of length c and two equal axes of length a, the lattice strain is given by $\varepsilon_0 = (c - a)/a$. In a rhombohedral crystal, ε_0 is the magnitude of the lattice shear strain relative to the cubic state. It is necessary to specify the critical driving force G_c at the onset of switching (analogous to yield stress in plasticity). In principle, G_c may take on distinct values for each transformation system. For simplicity, the values of G_c for each system are assumed to be identical. Thus, G_c is assumed to be the work dissipated in moving *any* domain wall through a unit volume of material. It is convenient to consider the special case of 180° switching under electric field E_0 which transforms the remanent polarization by $2P_0$ in the direction of the applied field, but leaves the remanent strain unchanged. Then $2E_0 P_0 = G_c$ and the critical driving force may be specified in terms of the electric field E_0. Finally, a value of the hardening parameter h is needed; as discussed above, the calculations in the present study are an approximation to non-hardening behaviour with $h \to 0$. Thus the three scalar parameters P_0, ε_0 and E_0 are sufficient to define the nonlinear crystal response.

(iii) The set of domain orientations and transformations. In the present model the crystal structure is specified by the set of polarization directions $\mathbf{n}$ of the variants. Tetragonal crystals are simulated using the set of six directions $\mathbf{n}$ in the $\langle 1\ 0\ 0 \rangle$ family. There are then six $\boldsymbol{\varepsilon}_I$ and six corresponding $\mathbf{P}_I$. The set of transformations which may operate is the 30 possible transformations which convert variant J to variant I where $I, J = 1, \ldots, 6$ with $I \neq J$. In Section 3.2 the consequence of freezing (i.e., switching off) a subset of transformation systems is explored. Disallowing the transformation of material of type J to type I is a way of modelling the absence of a mobile domain wall separating variants I and J. In Section 3.2 the tetragonal system is also compared with a trigonal (or rhombohedral) system where the polarization directions are given by the 8 members of the $\langle 1\ 1\ 1 \rangle$ family, and there are then 56 transformations.

The model parameters are thus the six scalars μ, κ, d_{33}, E_0, P_0, ε_0, and the set of domain orientations and transformations. For convenience, define the combined quantities $\tau_0 = E_0 \sqrt{\kappa \mu}$ with dimensions of stress, $D_0 = E_0 \kappa$ with dimensions of electric displacement, and $\gamma_0 = E_0 \sqrt{\kappa/\mu}$ with dimensions of strain. Note that τ_0 is not a measure of the switching stress, but rather a measure of the coercive field strength in units of stress. The six scalar parameters may then be reduced to the three non-dimensional quantities:

$$d^* = d_{33}\sqrt{3\mu/\kappa}, \tag{23}$$

$$P^* = P_0/D_0, \tag{24}$$

$$\varepsilon^* = \varepsilon_0/\gamma_0. \tag{25}$$

Here, d^* characterises the strength of electromechanical coupling, while P^* and ε^* characterise the magnitude of the dielectric and the ferroelastic nonlinearity, respectively.

3.1. Influence of the linear and nonlinear material parameters

The effect of varying each of the three non-dimensional parameters d^*, P^* and ε^* is now explored for a tetragonal crystal system with 6 variants and 30 transformations. The parameters are varied about a set of nominal values $d^* = 0.7$, $P^* = 20$ and $\varepsilon^* = 5$ which give ferroelectric behaviour similar to that of typical PZT-type materials. In all calculations the initial state is an

unpoled polycrystal with 1/6 of the volume fraction of each grain in each of the six crystal variants. Self-consistent averaging is used with 100 grains, uniformly distributed in orientation. In each calculation, the non-dimensional electrical load E_3/E_0 is increased from zero to 10 and then decreased back to zero. This loading history corresponds to poling the polycrystal with a quarter cycle of electric field loading, and is of practical relevance to the industrial poling process. Experimental data already exists for this loading case and an explicit comparison with the model is made in Section 4. Additionally, it is instructive to determine how the qualitative predictions of the model depend upon the input parameters.

First, consider the influence of d^* on the predicted response. The model response in terms of P_3^r/P_0 and $\varepsilon_{33}/\varepsilon_0$ versus E_3/E_0 is shown in Fig. 1, for d^* varying in the range $0.01 \leqslant d^* \leqslant 1$. Values of d^* greater than about 0.1 indicate significant piezoelectric coupling. A consequence is that interaction stresses arise due to mismatch in piezoelectric properties between each grain and the effective medium in which it is embedded. The effect of increasing d^* is to suppress 90° switching. Notice that when $E/E_0 < 1.4$ the polarization response is independent of the value of d^*: the field strength is insufficient to activate 90° switching, so that only 180° systems operate. These are strain free, and are thus not affected by interaction stresses. Saturation limits in Fig. 1 show the levels of remanent polarization and strain which would be reached by full switching; these levels are not achieved for practical poling fields. It is noted in passing that, at an applied electric field of magnitude E_0, interaction stresses due to grain by grain variation in remanent strain are comparable in magnitude to the interaction stresses due to the linear piezoelectric effect when d^* is of similar magnitude to ε^*.

Fig. 2 shows the effect of varying P^* over the range $P^* = 1$ to 100. When $P^* = 1$ the magnitude of the remanent polarization and the linear dielectric effect are approximately equal at electric fields of order E_0. Practical ferroelectrics typically possess a P^* of 5 or more. For a sufficiently small value of P^* (in the present simulations $P^* = 1$ is sufficient) there is negligible
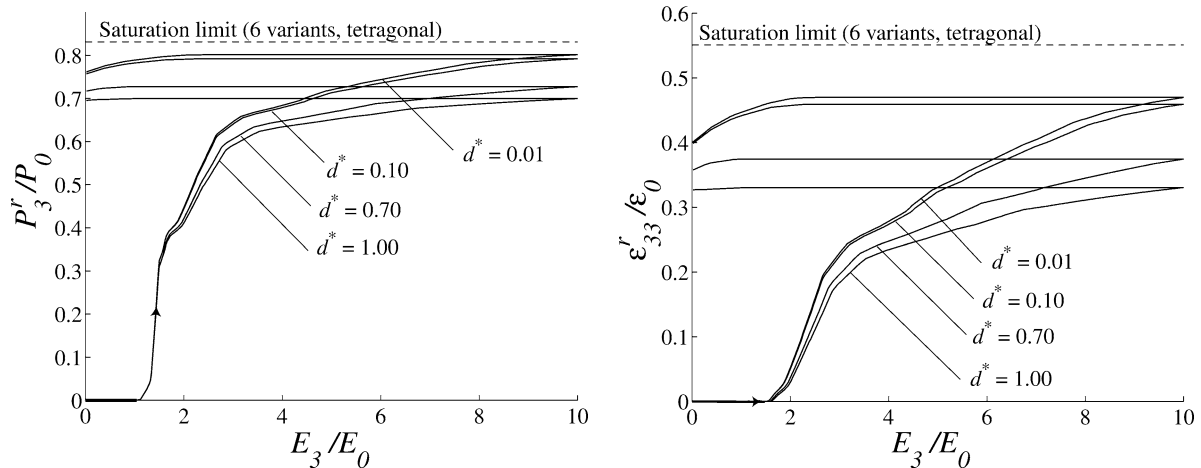

Fig. 1. The effect of varying d^* on model response, holding $P^* = 20$ and $\varepsilon^* = 5$.
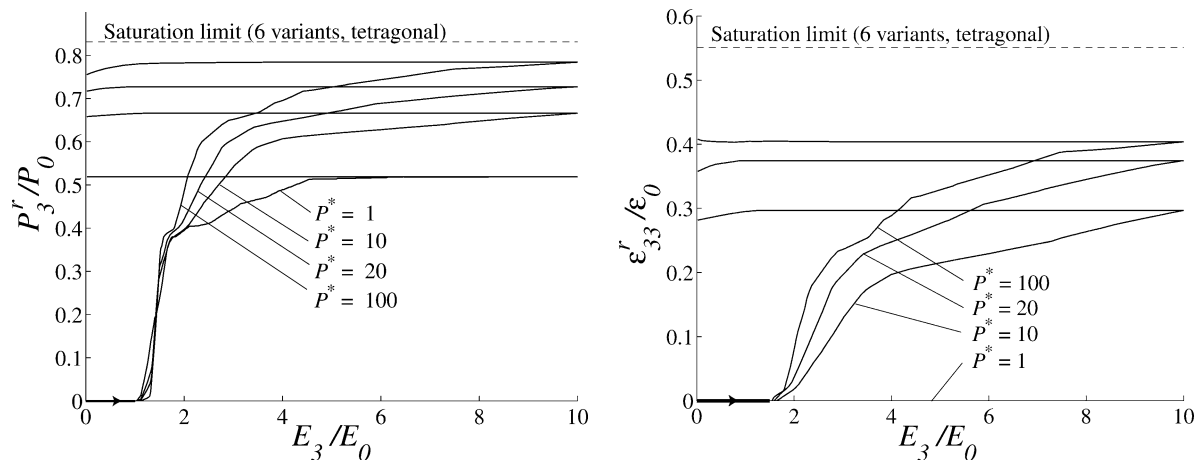

Fig. 2. The effect of varying P^* on model response, holding $d^* = 0.7$ and $\varepsilon^* = 5$.

90° switching and consequently no remanent straining occurs. The explanation is that the work done by external loads during a 90° switch is insufficient to balance the increase in elastic energy corresponding to local interaction stresses. To understand this sudden collapse of strain response, consider the interaction fields arising in the self-consistent scheme. In order to simplify matters, consider the approximate switching criterion of Hwang et al. (1998) for a single, spherical domain in an infinite matrix with linear elastic and dielectric behaviour:

$$\left[\boldsymbol{\sigma} - \frac{2\mu(7-5\nu)}{15(1-\nu)}\left(\boldsymbol{\varepsilon} - \boldsymbol{\varepsilon}_\mathrm{m} + \frac{\Delta\boldsymbol{\varepsilon}}{2}\right)\right] \cdot \Delta\boldsymbol{\varepsilon} + \left[\mathbf{E} - \frac{1}{3\kappa}\left(\mathbf{P} - \mathbf{P}_\mathrm{m} + \frac{\Delta\mathbf{P}}{2}\right)\right] \cdot \Delta\mathbf{P} \geqslant 2E_0 P_0. \tag{26}$$

Here $\boldsymbol{\sigma}$ and $\mathbf{E}$ are the remotely applied stress and electric field, $\boldsymbol{\varepsilon}_\mathrm{m}$ and $\mathbf{P}_\mathrm{m}$ are the remanent strain and polarization in the infinite matrix, $\boldsymbol{\varepsilon}$ and $\mathbf{P}$ are the remanent strain and polarization of the domain and $\Delta\boldsymbol{\varepsilon}$ and $\Delta\mathbf{P}$ are the finite changes in $\boldsymbol{\varepsilon}$ and $\mathbf{P}$ respectively, upon switching. Consider the incremental switching of the spherical inclusion by the operation of a single switching system α. Neglecting second order terms in Eq. (26) and setting $\nu = 1/3$ gives:

$$\left[\boldsymbol{\sigma} - \frac{16\mu}{15}(\boldsymbol{\varepsilon} - \boldsymbol{\varepsilon}_m)\right] \cdot \Delta\boldsymbol{\varepsilon}_\alpha + \left[\mathbf{E} - \frac{1}{3\kappa}(\mathbf{P} - \mathbf{P}_m)\right] \cdot \Delta\mathbf{P}_\alpha \geqslant 2E_0 P_0. \tag{27}$$

This incremental switching criterion assumes that each grain is constrained by a linear elastic and dielectric matrix, whereas in the self-consistent homogenisation, each grain is constrained by an effective medium with the tangent moduli of the polycrystal. During switching, the tangent moduli may soften by as much as an order of magnitude, reducing the effective μ and $1/\kappa$. However, the following argument is not affected by scaling μ and $1/\kappa$ by the same factor. Consider the inclusion and matrix having initially identical remanent strain and polarization; a single transformation system operates and transforms a volume fraction f of the inclusion. When the volume fraction f has transformed, the strain and polarization of the inclusion differ from those of the matrix by

$$\boldsymbol{\varepsilon} - \boldsymbol{\varepsilon}_m = f\Delta\boldsymbol{\varepsilon}_\alpha, \tag{28}$$

$$\mathbf{P} - \mathbf{P}_m = f\Delta\mathbf{P}_\alpha. \tag{29}$$

For a transformation system which converts the polarization direction from $\mathbf{n}_I$ to $\mathbf{n}_J$, we have

$$\Delta\boldsymbol{\varepsilon}_\alpha = 3\varepsilon_0(\mathbf{n}_J\mathbf{n}_J - \mathbf{n}_I\mathbf{n}_I)/2, \tag{30}$$

$$\Delta\mathbf{P}_\alpha = P_0(\mathbf{n}_J - \mathbf{n}_I) \tag{31}$$

and this allows the switching criterion to be rewritten as

$$\frac{\boldsymbol{\sigma} \cdot (\mathbf{n}_J\mathbf{n}_J - \mathbf{n}_I\mathbf{n}_I)}{2\tau_0 P^*/3\varepsilon^*} + \frac{\mathbf{E} \cdot (\mathbf{n}_J - \mathbf{n}_I)}{E_0} \geqslant 2 + f\left(\frac{24(\varepsilon^*)^2}{5P^*}\left(1 - (\mathbf{n}_I \cdot \mathbf{n}_J)^2\right) + \frac{2P^*}{3}(1 - \mathbf{n}_I \cdot \mathbf{n}_J)\right). \tag{32}$$

For 180° switching $\mathbf{n}_J = -\mathbf{n}_I$ and the switching criterion collapses to

$$\frac{\mathbf{E}}{E_0} \cdot \mathbf{n}_J \geqslant 1 + f\left(\frac{2P^*}{3}\right) \tag{33}$$

whilst for 90° switching $\mathbf{n}_J \cdot \mathbf{n}_I = 0$ and

$$\frac{\boldsymbol{\sigma}}{2\tau_0 P^*/3\varepsilon^*} \cdot (\mathbf{n}_J\mathbf{n}_J - \mathbf{n}_I\mathbf{n}_I) + \frac{\mathbf{E}}{E_0} \cdot (\mathbf{n}_J - \mathbf{n}_I) \geqslant 2 + f\left(\frac{24(\varepsilon^*)^2}{5P^*} + \frac{2P^*}{3}\right). \tag{34}$$

The operation of a single 90° switching system produces a change in both remanent strain and polarization. However, the simultaneous operation of two distinct 90° systems can give rise to polarization with no remanent strain change. This happens if $\mathbf{n}_I(2) = -\mathbf{n}_J(1)$ and $\mathbf{n}_J(2) = -\mathbf{n}_I(1)$, where the labels (1) and (2) refer to the two distinct switching systems. Equally, remanent strain can arise with no polarization change if $\mathbf{n}_I(2) = -\mathbf{n}_I(1)$ and $\mathbf{n}_J(2) = -\mathbf{n}_J(1)$. In either case, the switching criteria for the two systems acting simultaneously can be combined; the two cooperative systems may then be treated as a single switching system. In the case of strain-free, cooperative 90° switching, this gives:

$$\frac{\mathbf{E}}{E_0} \cdot (\mathbf{n}_J - \mathbf{n}_I) \geqslant 2 + 2f\left(\frac{2P^*}{3}\right), \tag{35}$$

where $\mathbf{n}_I = \mathbf{n}_I(1)$ and $\mathbf{n}_J = \mathbf{n}_J(1)$. Comparing Eqs. (35) and (34) shows that under purely electrical loading, a smaller electric field is needed to drive cooperative 90° switches than that needed for the individual 90° switching systems, provided $\varepsilon^*/P^* > 0.37$. Electrical loading does not produce remanent strain under these conditions, as seen in Fig. 2, for the case $\varepsilon^* = 5$ and $P^* = 1$. Similarly, when ε^* is varied in the range 1 to 100, as shown in Fig. 3, with P^* held fixed at 20, remanent straining is
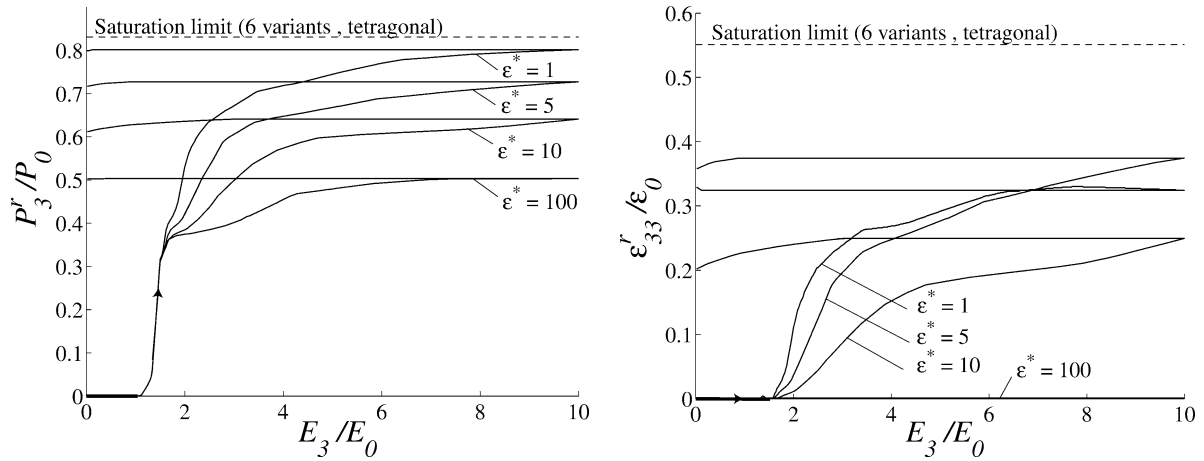
Fig. 3. The effect of varying ε^* on model response, holding $P^* = 20$ and $d^* = 0.7$.
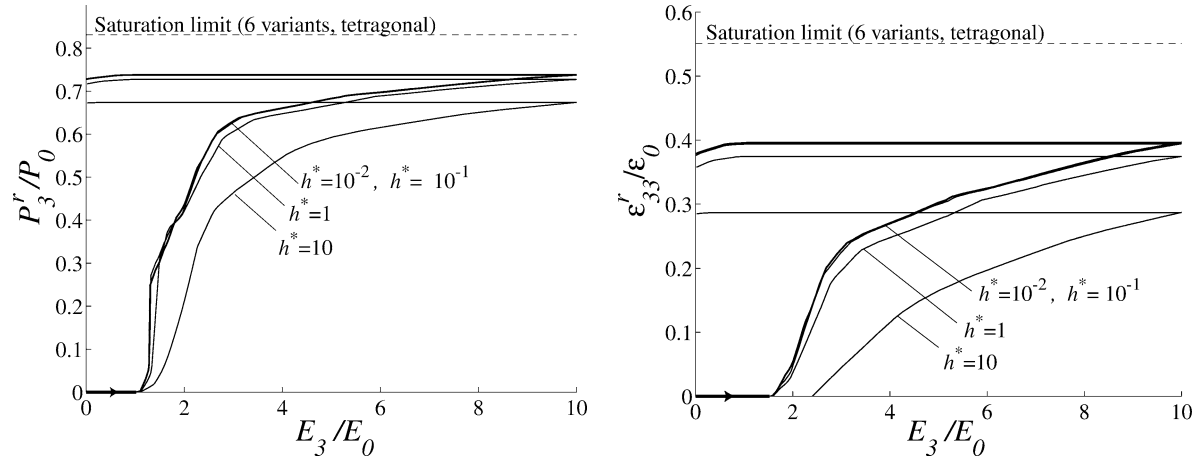

Fig. 4. The effect of varying h^* on model response, with $P^* = 20$, $\varepsilon^* = 5$ and $d^* = 0.7$.

suppressed when $\varepsilon^* \geqslant 10$. This behaviour is consistent with the observation by Arlt (1996b), that 90° switching processes may occur in laminar stacks of domains in such a way as to produce 180° switching as their net effect. The above argument, based on the model of Hwang et al. (1998) neglects piezoelectric interactions. Nevertheless, it is clear that the qualitative behaviour is strongly dependent upon the dimensionless parameters ε^* and P^*.

Typical ferroelectric ceramics have $\mu \sim 20$ GPa, $\kappa \sim 1.50 \times 10^{-8}$ F·m^{-1}, $\varepsilon_0 \sim 1\%$, $P_0 \sim 0.35$ C·m^{-2}. Thus, the ratio ε^*/P^* is approximately 0.5, indicating that relatively small changes in material properties would allow or suppress remanent straining under electrical load. Surprisingly, this result is independent of the single crystal coercive field E_0.

As a final comparison, consider the effect of varying the hardening rate h, as defined by Eq. (15). In the limit $h \to 0$ the tangent moduli of Eq. (21) become infinite whenever switching occurs. Note that h may be normalised by the initial value of G_c, which for 180° switching is $2E_0 P_0$; thus define the non-dimensional measure $h^* = h/(2E_0 P_0)$. When h^* equals unity the complete transformation of a ferroelectric grain from one crystal variant to another requires a doubling of the coercive field. Fig. 4 shows the effect of varying h^* over the range 0.01–10. The response becomes insensitive to h^* for $h^* < 0.1$. However, with h^* close to zero, very small load steps are needed for accurate calculation of the nonlinear response. A practical compromise is used in the subsequent calculations: h^* is set to unity, while the increments $\dot{G}_c$ are relaxed to zero. This allows for the rapid calculation of material response at the cost of a small compromise in accuracy.

3.2. Influence of the set of switching systems

The set of available transformations in a ferroelectric polycrystal governs the nonlinear response in a manner analogous to the effect of slip-systems on the plastic response of a polycrystal. If there is an insufficient number of switching systems, mismatches in strain and polarization between each grain and the surrounding medium result, and this produces interaction stresses and electric fields. Additionally, if there are only a few switching systems in each crystal, the coercive field and stress levels become strongly dependent on crystallographic orientation. In a random polycrystal this causes a smearing effect, whereby grains transform over a wide range of values of the applied field.

In the following discussion, four distinct arrangements of the set of transformation systems are compared. In each case the transformation systems are specified by defining the set of polarization directions **n** which a domain may adopt. The critical driving force G_c is assumed to be identical for all transformations. The systems considered are:

1. A system with 8 polarization directions **n** in the $\langle 1\,1\,1 \rangle$ family. This system corresponds to the trigonal (or rhombohedral) phases found in many perovskite ferroelectrics. Transformation between variants is by 70.6°, 109.4° or 180° switching.
2. A system with 6 polarization directions **n** in the $\langle 1\,0\,0 \rangle$ family of directions. This corresponds to the tetragonal phase in perovskite ferroelectrics. Transformation is by 90° or 180° switching.
3. A reduced tetragonal system with 4 vectors **n**, given by [1 0 0], [–1 0 0], [0 1 0] and [0 –1 0] in local coordinates. This corresponds to a crystal in the tetragonal phase with only 4 crystal variants present, their polarization vectors lying in a plane. Transformation is by 90° or 180° switching.
4. A reduced tetragonal system with 2 vectors **n**, given by [0 0 1], [0 0 –1] in local coordinates. This corresponds to a crystal with only 2 variants present, admitting 180° switching only. Crystals with a domain structure consisting of a stack of alternating layers of 2 crystal variants are commonly found in ferroelectrics.

Consider poling of a randomly oriented polycrystal with a large number of grains, by applying an electric field E_3 of sufficient magnitude to give almost complete switching. Many domains are imperfectly aligned with the applied poling field, and consequently the saturation polarization P_3^r for the polycrystal will not reach P_0. Calculated values for the saturation polarization of the polycrystal for each of the 4 systems described above are given in Table 1. Similarly, the saturation value of remanent strain ε_{33}^r during poling is less than ε_0, as shown in Table 1. However, the saturation conditions are achieved only at very high levels of applied loading (Landis et al., 2003); full saturation is not normally achieved during poling. The saturation value of remanent strain ε_{33}^r under electric field loading is equivalent to the ε_{33}^r value produced by loading with a uniaxial tensile stress σ_{33}. Here again, full strain saturation is unlikely to be achieved in practice due to fracture prior to complete switching. Note that the saturation strain in tension is distinct from that in compression. Values given in Table 1, are for crystals with $c > a$. For the case $c < a$, the values of normalised polarization P_3^r / P_0 in Table 1 are unchanged; the normalised values of saturation strain are obtained immediately by exchanging the values for tension and compression.

Table 1 also shows the number of linearly independent components of remanent strain and polarization which may be generated within each crystal system. For example, in the tetragonal system with 6 variants such that the directions **n** are in the $\langle 1\,0\,0 \rangle$ family, it is possible by combining arbitrary volume fractions of each variant to produce a volume average polarization which lies in any given direction in 3 dimensions. Thus the system can produce 3 independent polarization components. In general, the set of M distinct crystal variants gives M distinct vectors in 3 dimensions, which may be arranged into an $M \times 3$ matrix whose rank is the number of linearly independent polarization components. The number of independent strain components may similarly be calculated. Any crystal with at least 3 independent polarization components and 5 independent strain components is capable of adopting the macroscopic values of remanent strain and polarization, regardless

Table 1

Axial saturation values of remanent strain and polarization for various crystal systems. Notes: (a) exact value is $\sqrt{2}/2$ (b) exact value is $1/\pi$

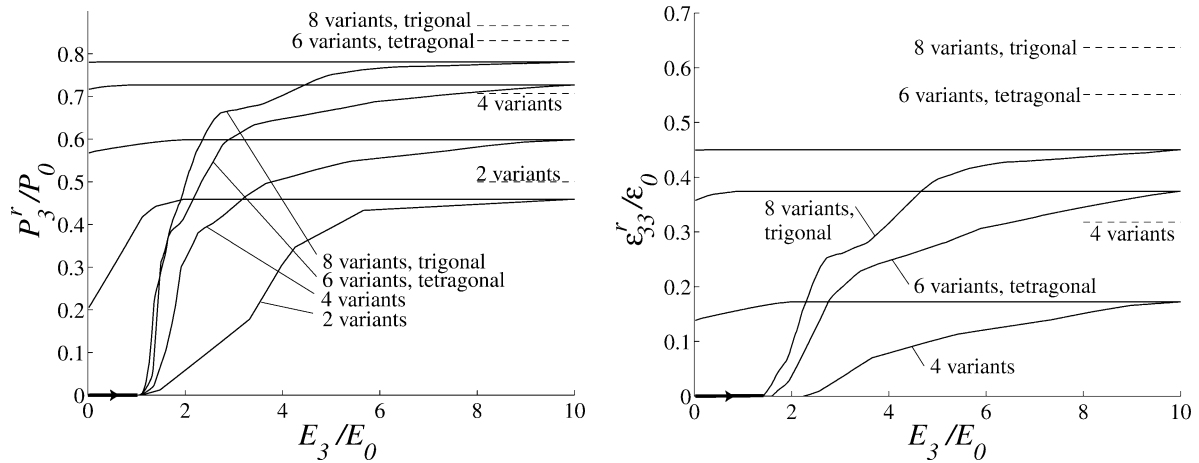| Value	Loading	Crystal system			
		Trigonal (8 variant)	Tetragonal (6 variant)	Tetragonal (4 variant)	(2 variant)
P_3^r / P_0	E_3	0.87	0.83	0.71[a]	0.50
$\varepsilon_{33}^r / \varepsilon_0$	E_3 or σ_{33} tensile	0.64	0.55	0.32[b]	0
$\varepsilon_{33}^r / \varepsilon_0$	E_3 or σ_{33} compressive	−0.43	−0.40	−0.32	0
Independent remanent strains		3	2	1	0
Independent remanent polarizations		3	3	2	1

Fig. 5. The effect of distinct crystal systems on model response. Saturation limits are shown as dashed lines. In each case, $P^* = 20$, $\varepsilon^* = 5$ and $d^* = 0.7$.

of its orientation. Failure to satisfy these conditions results in mismatches between the remanent state of the grain and that of the effective medium.

Fig. 5 shows the model response of the 100 grain polycrystal to poling with an applied electric field E_3 for each of the four crystal systems described above. The material parameters are identical in each simulation, with $P^* = 20$, $\varepsilon^* = 5$ and $d^* = 0.7$. Note that the crystal systems with only 2 or 4 variants show significant switching during unloading of the electric field, due to strong interaction fields. The presence of 6 or 8 variants reduces the mismatch in remanent quantities between individual grains and the polycrystal, and so reduces the interaction fields to the extent that only slight non-linearity occurs during unloading.

So far, the self-consistent calculations relate to a polycrystal in which all grains have the same arrangement of switching systems. In industrially relevant ferroelectrics, a mixture of grains with distinct switching systems can be present in the same polycrystal. This may be modelled by taking the self-consistent average response of the set of grains, with a given volume fraction of each type of the crystal system. A wide variety of material behaviour may be thereby reproduced. In Section 4 this method is used to fit the self-consistent model to the response of three materials under combined stress and electric field in proportional loading. The trigonal phase (8 variants) exists in PZT materials, and some predictions for this system are given in Fig. 5, but when calibrating the model in this study, the trigonal phase is neglected for simplicity. Thus, in calibrating the model against measured data, it is assumed that the polycrystal contains a volume fraction f_i of tetragonal material with i variants ($i = 2, 4, 6$) and f_0 of linear dielectric material.

4. Comparison of measured data with model behaviour under proportional loading

4.1. Qualitative comparison

A systematic study of switching behaviour in PZT-5H, PZT-4D and Barium Titanate under both proportional and non-proportional loading has been conducted recently (Shieh, 2003; Huber et al., 2002). The proportional loading measurements from that study are here modelled using the self-consistent micromechanics model described in Section 2. In the proportional loading tests, each material was initially in an isotropic, unpoled state and was loaded with uniaxial compressive stress σ_{33} and a proportional electric field E_3 parallel to the axis of the stress. The loading was carried far into the nonlinear regime for each material. The loading paths in stress-electric field space are shown in Fig. 6; in each case the material was loaded at constant rate along a path such as OA and then unloaded at the same rate. The entire loading cycle was carried out in 30 s. The resulting material responses in electric displacement versus electric field and stress are shown in Fig. 7. Note that no response to loading path OG is shown as loading by a purely compressive stress from the isotropic state does not produce electric displacement; this observation is readily explained by a symmetry argument.

In order to model the family of data shown in Fig. 7, it is necessary to select appropriate model parameters. It is immediately evident that the material responses are qualitatively similar. For each material, a superimposed compressive stress had relatively little effect on the electric displacement at electric fields well below the coercive field, but always reduced the peak electric displacement reached. This suggests that in the early stages of switching, the nonlinear response is dominated by switching systems which are insensitive to applied stress – these are the 180° systems and strain-free cooperative 90° systems. This feature
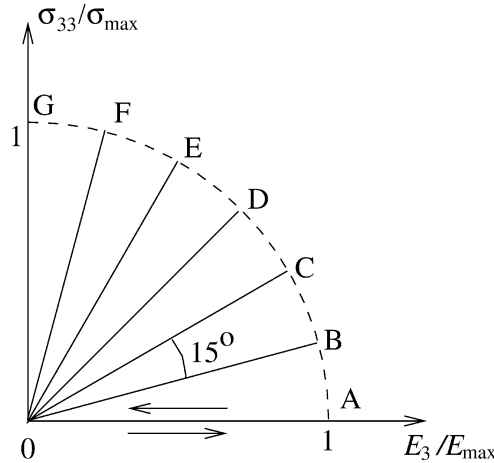
Fig. 6. Loading paths for proportional loading with uniaxial compressive stress σ_{33} and electric field E_3 (see Shieh, 2003 for details). For PZT-5H the peak electric field load value was $E_{max} = 1.5$ MV·m^{-1} and the peak stress value was $\sigma_{max} = 300$ MPa. For PZT-4D the corresponding values were $E_{max} = 5.0$ MV·m^{-1}, $\sigma_{max} = 500$ MPa. For Barium Titanate the load values were $E_{max} = 3.25$ MV·m^{-1}, $\sigma_{max} = 400$ MPa.

can be illustrated by constructing offset switching surfaces for the three materials in the in the $(\boldsymbol{\sigma}, \mathbf{E})$ loading space (Shieh, 2003). The switching surfaces consist of the locus of points at which the difference in electric displacement from the initial linear response reaches a fixed offset value. Fig. 8 shows offset switching surfaces for each material in (σ_{33}, E_3) space, corresponding to offsets in D_3 of 4%, 12% and 40% of the saturation value, P_r, reached under purely electrical loading. At large offsets, such as 40% P_r, the material has reached a partially poled state, and piezoelectric effects contribute to the electric displacement offset, in addition to the remanent polarization. In both PZT-4D and Barium Titanate the switching surfaces for small offsets are close to straight lines parallel to the stress axis: the onset of switching is almost independent of the applied stress.

A switching response that is independent of stress is suggestive of 180° switching, assuming that normality holds. The data shown in Fig. 7 reveal that, after initial switching, the D_3–E_3 response is sensitive to the compressive stress level. These observations suggest that both 90° and 180° switching are present, with 180° switching dominating the behaviour at low load levels. In the self-consistent model, these features are captured by having a high volume fraction f_2 of material in which switching is by 180°, the remaining volume fraction comprising material capable of both 90° and 180° switching.

The data for PZT-4D and Barium Titanate display a reversal of switching upon unloading from the poled state (see Fig. 7). A comparison with Fig. 5 suggests that these materials should be modelled with a high volume fraction of material containing only a single switching system. This is consistent with the use of a high volume fraction f_2 in these two materials. Conversely, in PZT-5H there is little reversal of switching upon unloading and so material with multiple switching systems is needed in the model (high values of f_4 or f_6).

4.2. Calibration of the model

Particular values of material parameters in the self-consistent model are now chosen for the three ceramics Barium Titanate, PZT-4D and PZT-5H, in turn.

4.2.1. Barium Titanate

Approximate values for the shear modulus μ, piezoelectric coefficient d_{33} and dielectric permittivity κ and coercive field E_0 for Barium Titanate are taken from manufacturer's data and values from similar materials reported in the literature. Similarly, values for the remanent polarization P_0 and lattice strain ε_0 of tetragonal Barium Titanate single crystals are readily available (see Table 2). These values give $d^* = 0.45$, $\varepsilon^* = 32.7$, $P^* = 45$, $\varepsilon^*/P^* = 0.73$. To complete the specification, Barium Titanate is treated as a composite comprising 25% of four-variant material, 60% of two-variant material, and 15% of dielectric inclusions ($f_4 = 0.25$, $f_2 = 0.6$, and $f_0 = 0.15$). Fig. 7 indicates that the remanent polarization after cold poling is only $0.21P_0$, consistent with the operation of only a single 180° switching system in each grain (see Fig. 5). This motivates the choice of a high volume fraction f_2 of two-variant material. A proportion $f_4 = 0.25$ is taken to provide some 90° switching. The modelled response of Barium Titanate to combined compressive stress and electric field is shown in Fig. 9. The model results were produced by self-consistent averaging over three sets of 100 grains, with the three sets corresponding to material of 4, 2, and 0 crystal variants. Each set of 100 grains is arranged with orientations in an approximately isotropic distribution and the initial
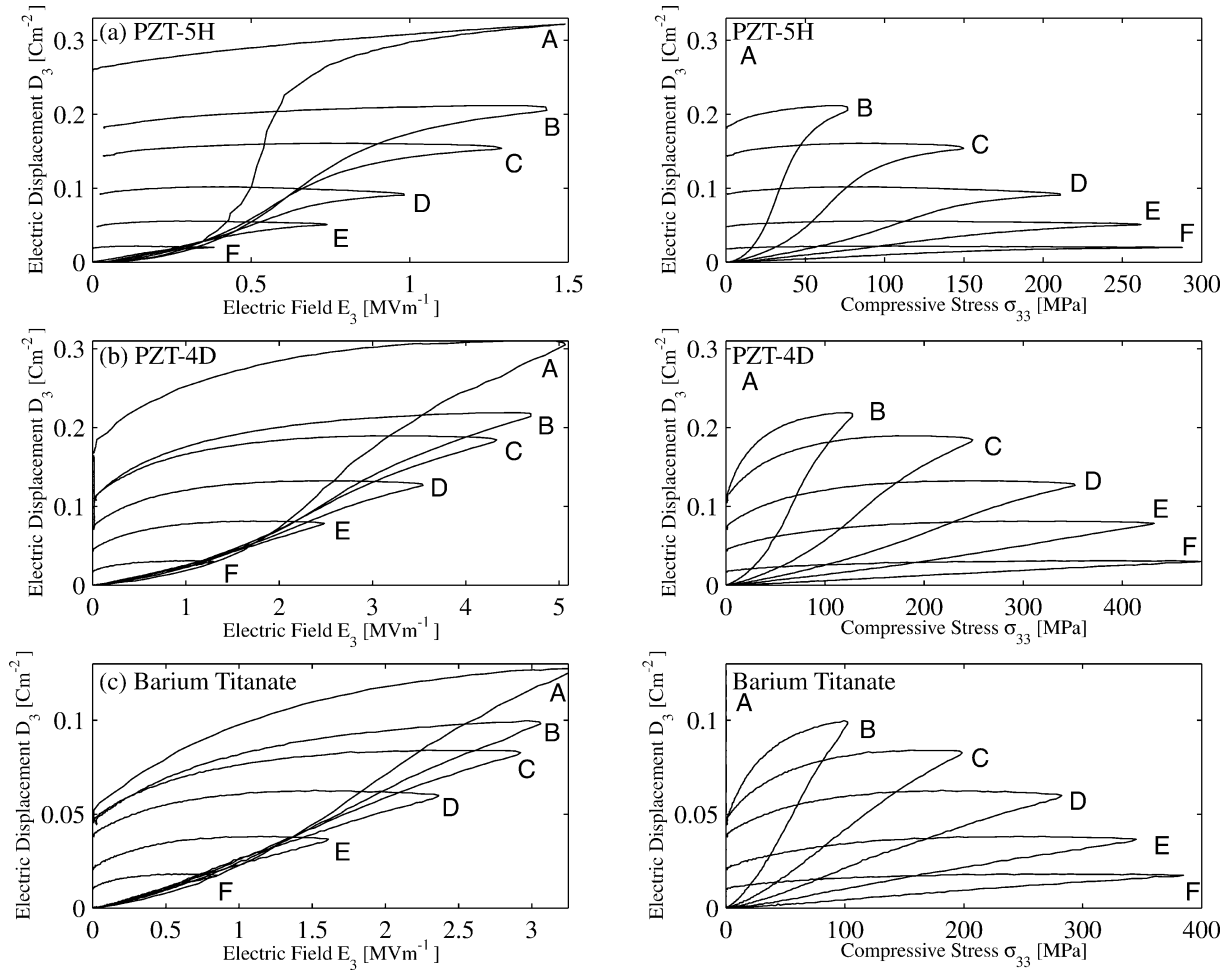
Fig. 7. Measured responses to a proportional loading test with uniaxial stress and electric field for (a) PZT-5H, (b) PZT-4D and (c) Barium Titanate. In each case the figure shows the electric displacement D_3 versus electric field E_3, and the corresponding D_3 versus stress σ_{33} response. The stress and electric field loads follow the paths A–G shown in Fig. 6.
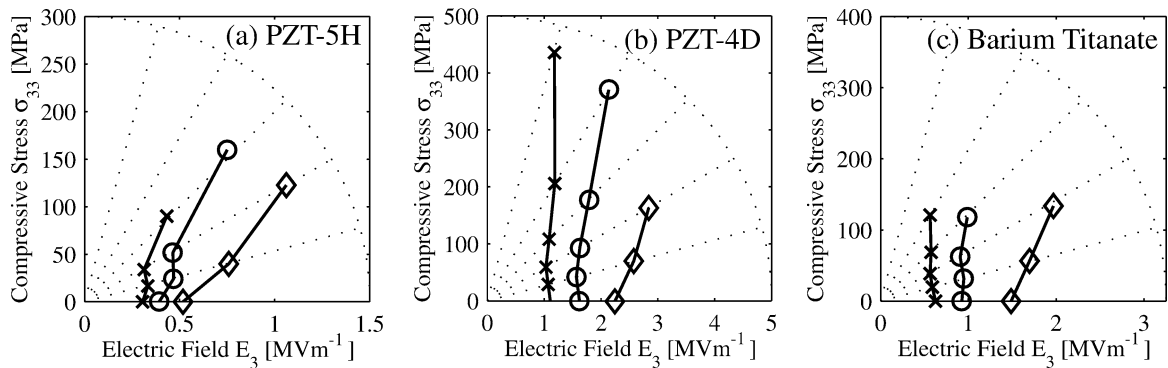

Fig. 8. Offset switching surfaces under proportional loading with uniaxial stress and electric field for (a) PZT-5H, (b) PZT-4D and (c) Barium Titanate, corresponding to the responses shown in Fig. 7. In each case the switching surfaces are for offsets of 4% (marked '×'), 12% (marked '○') and 40% (marked '◇') of the remanent polarization P_r after cold poling.

Table 2
Model parameters for PZT-5H, PZT-4D and Barium Titanate

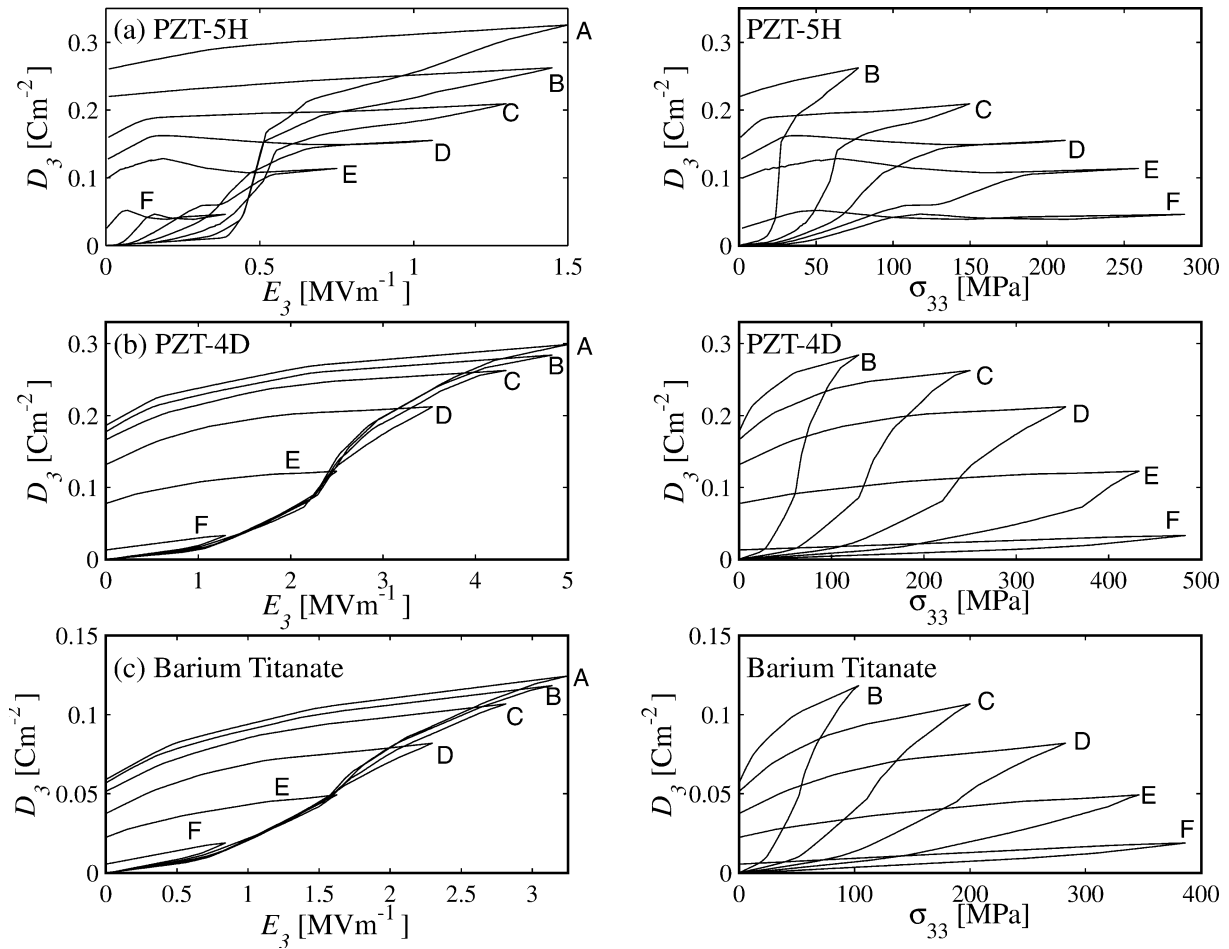| Parameter	PZT-5H	PZT-4D	Barium Titanate
μ [GPa]	21	32	48
d_{33} [pm·V^{-1}]	600	290	127
κ [nF·m^{-1}]	29	11.5	11.5
P_0 [C·m^{-2}]	0.65	0.6	0.26
ε_0 [%]	1.0	2.0%	0.8%
E_0 [MV·m^{-1}]	0.35	0.75	0.5
d^*	0.88	0.84	0.45
P^*	64	70	45
ε^*	24	45	32
Volume fraction f_6	0.60	0.00	0.00
Volume fraction f_4	0.00	0.25	0.25
Volume fraction f_2	0.40	0.75	0.60
Volume fraction f_0	0.00	0.00	0.15

Fig. 9. Modelled responses to a proportional loading test with uniaxial stress and electric field for (a) PZT-5H, (b) PZT-4D and (c) Barium Titanate. In each case the left-hand side figure shows the electric displacement D_3 versus electric field E_3, whilst the right-hand side figure shows the corresponding D_3 versus stress σ_{33} response. The stress and electric field loads follow the paths A–G shown in Fig. 6.
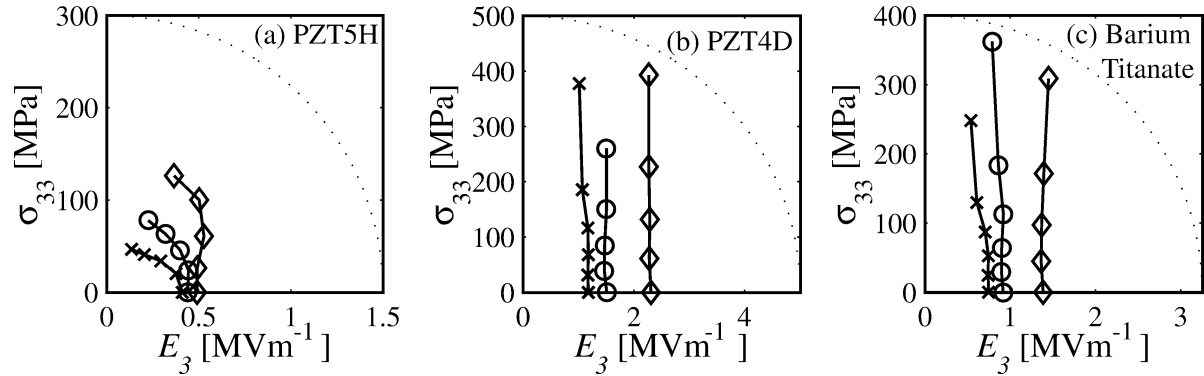
Fig. 10. Calculated offset switching surfaces under proportional loading with uniaxial stress and electric field for (a) PZT-5H, (b) PZT-4D and (c) Barium Titanate, corresponding to the model responses shown in Fig. 9. In each case the switching surfaces are for offsets of 4% (marked '×'), 12% (marked 'o') and 40% (marked '◇') of the remanent polarization P_r after cold poling.

state has equal volume fractions of material in each variant of each grain, giving zero initial remanent polarization in every grain.

4.2.2. PZT-4D

A similar approach to modelling PZT-4D results in the model parameters given in Table 2. Approximate values for the model parameters are taken from the manufacturer's data, but in this case, P_0 and ε_0 have been used as fitting parameters. As with Barium Titanate, it is found that switching is predominantly due to 180° systems and a substantial volume fraction $f_2 = 0.75$ of material containing only 2 variants is employed in the model. The modelled response to combined compressive stress and electric field (see Fig. 9) shows good agreement with the measured data in Fig. 7. Offset switching surfaces constructed from the modelled responses of PZT-4D and Barium Titanate are shown in Fig. 10, and give good agreement with the measured switching surfaces, for small offsets.

4.2.3. PZT-5H

It is observed that little or no reversal of switching occurs during unloading of PZT-5H. The material also retains a far greater remanent polarization than that of PZT-4D after cold poling. These observations, taken in the context of Fig. 5, suggest that a switching system with 6 or more variants dominates the behaviour. However, modelling PZT-5H using 100% of 6 variant material produces the effect that the onset of switching is very strongly dependent upon the applied compressive stress; this is inconsistent with the measured offset switching surfaces shown in Fig. 8. A compromise model with 60% by volume fraction of six-variant material, and 40% by volume fraction of two-variant material ($f_6 = 0.6$, $f_2 = 0.4$) provides a reasonable fit to the measurements of PZT-5H shown in Fig. 7. In calculating the modelled results shown in Fig. 9, the fit to measured data was improved by making the further assumption that, in the absence of applied stress, the first switches by 90° and 180° switching systems are activated at the same level of applied electric field. Thus, E_0 for 90° switching systems is set to be $1/\sqrt{2}$ of the value of E_0 for 180° systems. The modelled switching surfaces for PZT-5H in Fig. 10 show a significant stress dependence due to the presence of 90° switching. This occurs because a compressive stress provides a driving force for the operation of 90° systems and these can produce a change in polarization. However, the measured data show a converse effect where the compressive stress inhibits switching. This suggests that the order in which 90° switching systems operate differs between the model and the measurements; further work is needed to resolve this effect.

5. Conclusion

The ability of a self-consistent micromechanics model to reproduce the observed behaviour of three ferroelectric polycrystals has been explored. The non-dimensional parameters d^*, ε^*, and P^* are appropriate measures of the magnitude of electromechanical coupling, ferroelastic straining, and dielectric hysteresis. Materials with stable piezoelectricity must possess $d^* < 1$. A simplified model suggests that whenever $\varepsilon^*/P^* > 0.37$, interaction stresses strongly constrain 90° switching, and cooperative, strain-free switching dominates. In this case, materials may show substantial dielectric hysteresis, but relatively little remanent strain; strain produced during electrical loading is then principally due to the converse piezoelectric effect. Typical ferroelectric compositions have values of ε^*/P^* of order unity and consequently small changes in properties can have the effect of enabling or suppressing remanent strain during ferroelectric switching.

The self-consistent homogenisation allows the material response to be estimated for ferroelectric composites consisting of grains with distinct crystal systems. This feature is useful for estimating the material response when a volume fraction of material has its switching systems limited by the pinning of domain walls, or has purely dielectric behaviour. Using this approach it has been possible to reproduce with reasonable accuracy the material response of the three ceramics PZT-5H, PZT-4D and Barium Titanate. Approximate model parameters can be extracted from the measurement of linear moduli and the poling behaviour of each material. However, the particular model parameters used to reproduce the experimental data here are the outcome of a fitting procedure and, at present, no straightforward way to extract these model parameters directly from the measured data is known. The process of searching for appropriate model parameters is simplified somewhat by the introduction of appropriate non-dimensional groups, but remains problematic. This difficulty would be alleviated by the direct measurement of micromechanical parameters, such as the proportions of crystal variants present, their spontaneous strain and polarization states, and the linear moduli of individual domains.

Acknowledgement

References

Arlt, G., 1996a. A physical model for hysteresis curves of ferroelectric ceramics. Ferroelectrics 189, 103–119.

Arlt, G., 1996b. Switching and dielectric nonlinearity of ferroelectric ceramics. Ferroelectrics 189, 91–101.

Bassiouny, E., Maugin, G.A., 1989. Thermodynamical formulation for coupled electromechanical hysteresis effects-III. Parameter identification. Int. J. Engrg. Sci. 27 (8), 975–987.

Chen, X., Fang, D.N., Hwang, K.C., 1997. Micromechanics simulation of ferroelectric polarization switching. Acta Mater. 45 (8), 3181–3189.

Fan, J., Stoll, W.A., Lynch, C.S., 1999. Nonlinear constitutive behaviour of soft and hard PZT: Experiments and modeling. Acta Mater. 47 (17), 4415–4425.

Haug, A., Knoblauch, V., McMeeking, R.M., 2003. Combined isotropic and kinematic hardening in phenomenological switching models for ferroelectric ceramics. Int. J. Engrg. Sci. 41 (8), 887–901.

Hill, R., 1965. A self-consistent mechanics of composite materials. J. Mech. Phys. Solids 13, 213–222.

Huber, J.E., Fleck, N.A., 2001. Multi-axial electrical switching of a ferroelectric: theory versus experiment. J. Mech. Phys. Solids 49, 785–811.

Huber, J.E., Fleck, N.A., Landis, C.M., McMeeking, R.M., 1999. A constitutive model for ferroelectric polycrystals. J. Mech. Phys. Solids 47, 1663–1697.

Huber, J.E., Shieh, J., Fleck, N.A., 2002. Multi-axial response of hard and soft ferroelectrics under stress and electric field. Proc. SPIE 4699, 133–142.

Hwang, S.C., Huber, J.E., McMeeking, R.M., Fleck, N.A., 1998. The simulation of switching in polycrystalline ferroelectric ceramics. J. Appl. Phys. 84 (3), 1530–1540.

Hwang, S.C., Lynch, C.S., McMeeking, R.M., 1995. Ferroelectric/ferroelastic interactions and a polarization switching model. Acta Metallur. Mater. 43 (5), 2073–2084.

Kamlah, M., Jiang, Q., 1999. A constitutive model for ferroelectric PZT ceramics under uniaxial loading. Smart Mater. Structures 8, 441–459.

Kessler, H., Balke, H., 2001. On the local and average energy release in polarization switching phenomena. J. Mech. Phys. Solids 49 (5), 953–978.

Landis, C.M., 2002. Fully coupled, multi-axial, symmetric constitutive laws for polycrystalline ferroelectric ceramics. J. Mech. Phys. Solids 50, 127–152.

Landis, C.M., McMeeking, R.M., 2001. A self-consistent constitutive model for switching in polycrystalline Barium Titanate. Ferroelectrics 255, 13–34.

Landis, C.M., Wang, J., Sheng, J., 2003. Micro-electromechanical determination of the possible remanent strain and polarization states in polycrystalline ferroelectrics and the implications for phenomenological constitutive theories, in press.

Li, J., Weng, G.J., 1999. A theory of domain switch for the nonlinear behaviour of ferreoelctrics. Proc. Roy. Soc. London Ser. A 455, 3493–3511.

Lynch, C.S., 1998. On the development of multiaxial phenomenological constitutive laws for ferroelectric ceramics. J. Intell. Mater. Systems Structures 9, 555–563.

Michelitsch, T., Kreher, W.S., 1999. A simple model for the nonlinear material behaviour of ferroelectrics. Acta Mater. 46 (14), 5085–5094.

Shieh, J., 2003. Ferroelectrics: switching and cyclic behaviour. Ph.D. Dissertation. Univ. of Cambridge.

Shu, Y.C., Bhattacharya, K., 2001. Domain patterns and macroscopic behaviour of ferroelectric materials. Philos. Mag. B 81 (12), 2021–2054.